

# 电子束重熔对熔丝沉积钛合金 表面组织及性能的影响

迮颖<sup>1,2</sup>, 朱梦婷<sup>1,2</sup>, 孙世豪<sup>3,4</sup>, 陶学伟<sup>1,2</sup>, 张保森<sup>1,2</sup>, 姚正军<sup>3</sup>

(1.南京工程学院 材料科学与工程学院, 南京 211167; 2.江苏省先进结构材料与应用技术重点实验室, 南京 211167; 3.南京航空航天大学 材料科学与技术学院, 南京 210016;  
4.江苏集萃精密制造研究院有限公司, 南京 211800)

**摘要:** 目的 通过表面重熔处理解决沉积钛合金固有组织引起的表面磨损不均及摩擦不稳定的难题, 以拓宽沉积钛合金的应用领域。**方法** 采用电子束重熔工艺对熔丝沉积 Ti6Al4V 钛合金表面进行改性处理。利用体式显微镜、光学显微镜、X 射线衍射仪等分析重熔前后钛合金表层的宏观形貌、显微组织及物相组成变化, 运用纳米压痕仪及摩擦磨损试验机考察重熔层的表面纳米力学性能及耐磨性能, 并采用三维光学轮廓仪及扫描电子显微镜观察磨损形貌特征。**结果** 经电子束重熔处理后, 熔丝沉积钛合金沉积方向表面组织由不均匀的  $\alpha+\beta$  组成的网篮组织及魏氏组织转变为均匀分布的细针状马氏体 ( $\alpha'$ )。重熔处理试样表面纳米硬度均匀, 且得到明显提升, 达 3.8 GPa, 相较于未重熔试样提高了 15%以上, 表现出较高的硬弹性。重熔层具有稳定的摩擦系数和较优的耐磨性, 其平均摩擦系数为 0.45, 磨损率为  $3.59 \times 10^{-13} \text{ mm}^3/(\text{N}\cdot\text{m})$ , 相较于未重熔试样, 分别降低了 19.6% 和 22.1%, 其磨损机理以磨粒磨损、氧化磨损及粘着磨损为主。**结论** 电子束重熔工艺能够有效改善熔丝沉积钛合金沉积方向的表面组织均匀性, 可获得优异的表面力学性能及摩擦性能。

**关键词:** 电子束重熔; 熔丝沉积; 钛合金; 组织均匀性; 耐磨性

中图分类号: TH117 文献标识码: A 文章编号: 1001-3660(2023)04-0164-08

DOI: 10.16490/j.cnki.issn.1001-3660.2023.04.013

## Effect of Electron Beam Surface Remelting on Surface Microstructure and Properties of Wire-feed Additive Manufactured Titanium Alloy

ZE Ying<sup>1,2</sup>, ZHU Meng-ting<sup>1,2</sup>, SUN Shi-hao<sup>3,4</sup>, TAO Xue-wei<sup>1,2,\*</sup>, ZHANG Bao-sen<sup>1,2</sup>, YAO Zheng-jun<sup>3</sup>

(1. School of Materials Science and Engineering, Nanjing Institute of Technology, Nanjing 211167, China; 2. Jiangsu Key Laboratory of Advanced Structural Materials and Application Technology, Nanjing 211167, China; 3. School of Materials Science and Technology, Nanjing University of Aeronautics and Astronautics, Nanjing 210016, China; 4. JITRI Institute of Precision Manufacturing, Nanjing 211800, China)

收稿日期: 2022-04-05; 修订日期: 2022-07-28

Received: 2022-04-05; Revised: 2022-07-28

基金项目: 国家自然科学基金 (52005245); 江苏省大学生科技创新项目 (202011276069Y)

Fund: The National Natural Science Foundation of China (52005245); Innovation Training Program for College Students at Jiangsu Province (202011276069Y)

作者简介: 齐颖 (2000—), 女, 主要研究方向为表面工程。

Biography: ZE Yin (2000-), Female, Research focus: surface engineering.

通讯作者: 陶学伟 (1989—), 男, 博士, 讲师, 主要研究方向为金属先进制造及表面工程。

Corresponding author: TAO Xue-wei (1989-), Male, Doctor, Lecture, Research focus: advanced manufacturing and surface engineering of metal.

引文格式: 齐颖, 朱梦婷, 孙世豪, 等. 电子束重熔对熔丝沉积钛合金表面组织及性能的影响[J]. 表面技术, 2023, 52(4): 164-171.

ZE Ying, ZHU Meng-ting, SUN Shi-hao, et al. Effect of Electron Beam Surface Remelting on Surface Microstructure and Properties of Wire-feed Additive Manufactured Titanium Alloy[J]. Surface Technology, 2023, 52(4): 164-171.

**ABSTRACT:** Electron beam surface remelting is an advanced high-energy beam surface-modification technology that allows to locally manipulate the microstructure and performance without affecting the matrix material. It has attracted much attention for the fabrication of active and refractory materials, since a vacuum working environment can effectively avoid the introduction of extrinsic contaminants. The work aims to address the problems of insufficient wear resistance and friction instability resulted from the inherent microstructure of wire-feed additive manufactured titanium alloy through electron beam surface remelting to, broaden its application fields.

The square specimens ( $15 \text{ mm} \times 15 \text{ mm} \times 4 \text{ mm}$ ) were extracted from the electron beam free form fabricated Ti6Al4V alloy along the build direction. The polished specimens were treated by surface melting technique with an electron beam gun under a vacuum of  $10^{-3} \text{ Pa}$ , with fixed beam power of 180 W and moving speed of 5 mm/s. The overlap ratio between the two adjacent passes was 50%. The variation of macroscopic morphology, microstructure and phase composition of the titanium alloy before and after remelting were analyzed with stereomicroscope, optical microscope and X-ray diffractometer, respectively. The surface nanomechanical properties and wear resistance of the remelted layer were investigated with nanoindenter and wear testing machine, respectively. The worn features were characterized with three-dimensional optical profilometer and scanning electron microscope.

A favorable remelted layer was successfully prepared on the surface of deposited titanium alloy via electron beam surface remelting. Under the irradiation of electron beam, the as-received surface was melted completely into a molten pool, and then was rapidly solidified afterwards by self-quenching. Therefore, the initial heterogeneous microstructure (basket-wave structure and Widmanstatten structure composed of  $\alpha+\beta$ ) was transformed into homogeneous and fine acicular martensite ( $\alpha'$ ) after surface remelting treatment. The nanoindentation results showed that the remelted alloy provided a uniform and enhanced nanohardness (3.8 GPa), which was over 15% higher than that of the un-remelted sample, exhibiting a superior hard elasticity. The enhanced hardness was contributed to the formation of fine acicular martensite.

Due to the heterogeneous microstructure and insufficient hardness, a worn track with different degree of abrasion occurred easily on the surface of as-deposited alloy during the wear process. It resulted in the increase of roughness on the contact area between the alloy and counterpart, leading to the instability of friction and further deterioration of wear. As expected, a stable friction coefficient and a better wear resistance were available after surface remelting. The average friction coefficient was 0.45 and the wear rate was  $3.59 \times 10^{-13} \text{ mm}^3/(\text{N}\cdot\text{m})$ , which was 19.6% and 22.1% lower than that of the un-remelted one, respectively. The remelted layer possessed a superior tribological performance, which was attributed to its uniform microstructure and hard phase. Shallow grooves, minor adhesive traces and oxidation generated on its worn surface. The wear mechanism was not changed after the surface remelting treatment, and its dominant failure mechanism was abrasive wear, oxidation wear and adhesive wear.

This study shows that the microstructure homogeneity of wire-feed additive manufactured titanium alloy can be improved by electron beam surface remelting, and a favorable surface mechanical and tribological performance is achievable.

**KEY WORDS:** electron beam surface remelting; wire-feed additive manufacturing; titanium alloy; microstructure homogeneity; wear resistance

随着航空航天工业对轻量化要求的日益提高, 具有比强度高、耐蚀性好、耐热性优异的钛合金在航空航天装备上得到广泛应用<sup>[1-2]</sup>。熔丝沉积技术作为一种成本低、效率高、加工污染少的增材制造技术, 在大型复杂航空用钛合金结构件制造上展示出显著优势<sup>[3-4]</sup>。然而, 复杂的热循环致使成形件内部显微组织不均, 形成明显的层带结构 (Layer Banding)<sup>[3-6]</sup>。尽管成形件的整体力学性能能够满足使用要求, 但由于组织均匀性差, 在摩擦工况下, 极易造成钛合金成形件表面磨损不均, 引起摩擦不稳定而加剧磨损, 缩短了构件的服役寿命, 限制了熔丝沉积钛合金的工程应用。因此, 提高熔丝沉积钛合金表面的耐磨性, 并改

善性能均匀性是拓宽其应用范围的关键。

表面重熔技术是一种将金属表面局部加热熔化, 并快速凝固而获得均匀且细小晶粒组织的工艺手段, 具有工艺简单、基体材料不受限制、膜基结合优良等优点<sup>[7-13]</sup>, 在钛合金表面改性领域得到广泛关注。成前前等<sup>[8]</sup>研究了激光重熔处理对钛合金表面氮(氧)化层组织及性能的影响, 发现经激光重熔处理的改性层内部微观组织分布更均匀, 晶粒更细化, 且所制备的重熔层具有良好的硬弹性, 显著提升了 Ti6Al4V 表面的耐磨损能力。Yao 等<sup>[9]</sup>、Zhang 等<sup>[10]</sup>分别对 Ti-Zr 和 Ti-35Nb-2Ta-3Zr 钛合金表面进行了激光重熔处理, 发现重熔后的合金表层组织均匀, 且晶粒明显细

化,使钛合金的表面硬度提高了90%以上。叶秀等<sup>[11]</sup>利用重熔处理有效提高了激光选区熔化成形(SLM)Ti6Al4V钛合金的显微硬度及摩擦磨损性能。经激光重熔后,SLM成形件的显微硬度提高至444.0HV,摩擦系数降低至0.396。He等<sup>[12]</sup>采用激光重熔和时效处理在Ti-55511钛合金表面制备出由均匀纳米片层 $\alpha$ 相组成的改性层,显著改善了钛合金的表面硬度及耐磨性。Chen等<sup>[13]</sup>发现,Ti-36Nb-2Ta-3Zr-0.35O钛合金经电子束重熔后,其表层内部产生了大量弥散的针状 $\alpha''$ 相,表现出较高的硬度,且随着扫描速度提高, $\alpha''$ 相向 $\alpha'$ 相转变,进一步增强了合金的表面硬度及耐磨性。上述研究表明,表面重熔处理有利于优化钛合金表层组织分布、细化晶粒,显著改善合金的表面性能。尽管学者们利用重熔技术对增材制造钛合金表面进行改性处理,但主要探讨表层成分<sup>[14]</sup>、残余应力、表面形貌及粗糙度<sup>[15]</sup>等变化规律,较少关注重熔处理对增材制造钛合金层带结构的影响。

由于电子束重熔技术具有能量高、控制灵活等优点,且真空环境有效避免空气中有害杂质混入,特别适合钛合金等活性金属表面改性<sup>[6-7]</sup>。因此,本文利用电子束重熔技术对熔丝沉积Ti6Al4V钛合金进行表面处理,探讨了重熔处理对沉积体表层组织结构及硬度的影响,考察了重熔处理前后钛合金的摩擦行为,为解决熔丝沉积钛合金表面力学性能不均、局部磨损严重等问题和提升钛合金摩擦学适应性提供理论和实验依据,旨在拓宽熔丝沉积钛合金的应用领域。

## 1 试验

### 1.1 材料

试验材料选用自制的电子束熔丝沉积Ti6Al4V钛合金试样。熔丝沉积所用的进给材料为 $\phi 1.6$  mm Ti6Al4V合金丝材,沉积基板为锻造态Ti6Al4V钛合金,丝材及基板的化学成分见表1。沉积工艺参数:功率 $P=4.0$  kW、行进速度 $v=650$  mm/min、送丝速度 $v_w=3.5$  m/min、丝材进给角度为45°。沿着沉积方向(Z方向)从沉积钛合金上截取15 mm×15 mm×4 mm

的试样用于电子束表面重熔试验,如图1a所示。

**表1 熔丝沉积所用丝材及沉积基板的化学成分**  
**Tab.1 Chemical composition of wire and substrate used for wire-feed additive manufacturing**

	Al	V	O	C	N	H	Ti	wt.%
Wire	6.05	3.88	0.11	0.01	0.006	0.005	Bal.	
Substrate	6.12	3.95	0.12	<0.03	<0.02	0.009	Bal.	

### 1.2 电子束表面重熔方法

表面重熔处理前,先用砂纸去除试样表面氧化层,再用酒精超声清洗去除其表面污物。采用电子束成形设备对处理后的试样表面进行重熔处理,如图1b所示。具体工艺参数:电子束功率 $P=180$  W、扫描速度 $v=5$  mm/s、线能量密度为36 J/mm、真空度为 $10^{-3}$  Pa。采用搭接熔覆方式进行表面重熔处理,搭接率为50%,如图1c所示。

### 1.3 组织及性能表征

分别采用体视显微镜(SZN71)和光学显微镜(GX51)观察重熔层的宏观形貌及微观组织。利用X射线衍射仪(Ultima-IV)分析沉积钛合金重熔前后物相的变化。采用纳米压痕仪(G200)对重熔前后不同区域进行表面力学性能测试,测试条件:负载速率为100  $\mu$ N/s、最大载荷为100 mN、保压时间为10 s。每个区域测试20个点,取其平均值作为测试结果。采用万能摩擦磨损试验机(MFT-5000)考察试样的摩擦学行为,摩擦副为 $\phi 12.7$  mm  $\text{Si}_3\text{N}_4$ 陶瓷球。测试条件:法向载荷为10 N、频率为10 Hz、磨痕长度为2 mm、测试时间为10 min。利用三维光学轮廓仪(UP-3000)观测样品的磨损形貌及磨损体积,并计算磨损率 $\delta=V/F \cdot S^{[11]}$ 。其中,  $\delta$ 为磨损率,  $\text{mm}^3/(\text{N} \cdot \text{m})$ ;  $\Delta V$ 为试样磨损体积,  $\text{mm}^3$ ;  $F$ 为测试载荷 N;  $S$ 为摩擦滑动总路程, m。最后采用配备能谱仪(X-act one)的扫描电子显微镜(Merlin Compact)分析了磨损形貌及磨屑成分。

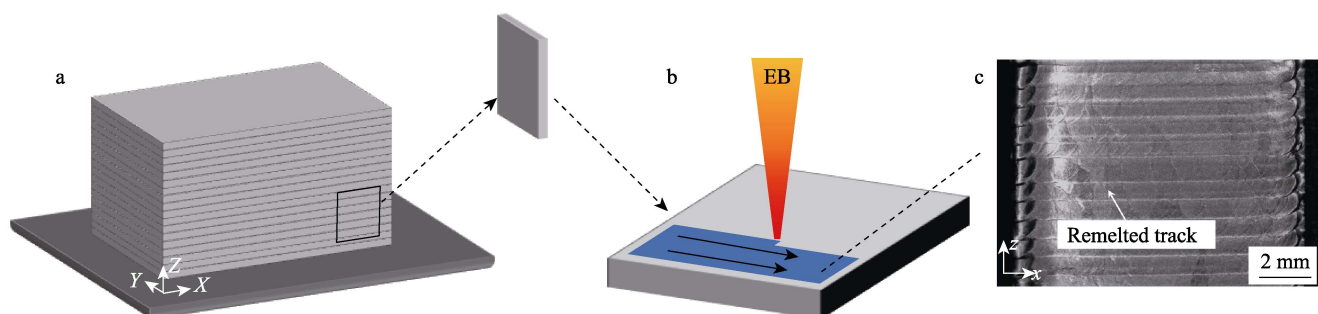


图1 取样示意图(a),电子束表面重熔示意图(b)和重熔层宏观照片(c)

Fig.1 Schematic diagram of sampling (a), schematic diagram of electron beam surface remelting (b), macrophotograph of remelted layer (c)

## 2 结果与讨论

### 2.1 显微组织及物相组成

熔丝沉积钛合金的宏观形貌及重熔前后的微观组织如图 2 所示。由图 2a 可见, 熔丝沉积钛合金内部存在由明暗相间条纹组成的层带结构。由图 3 所示的 XRD 分析结果可知, 明条纹与暗条纹区域均主要存在  $\alpha$  相和  $\beta$  相衍射峰, 其中明条纹区域的  $\beta$  相衍射峰更明显。通过金相分析可以发现, 明条纹主要由  $\alpha$  片层相对粗大且相互交织的网篮组织组成(见图 2b), 而暗条纹主要由  $\alpha$  片层相对细长且平行的魏氏组织组成 (见图 2c), 这是由沉积过程中复杂的热循环造成的。与激光快速成形不同, 电子束熔丝沉积过程中, 严重的热积累及真空环境使热散失减慢<sup>[5,16]</sup>, 导致熔池冷却相对缓慢, 主要发生  $\beta \rightarrow \alpha$  转变, 在中等冷却速度下得到魏氏组织<sup>[17]</sup>。由于暗条纹区域经历后续热循环时受热影响较小, 其显微组织及物相组成均不发生明显变化, 仍为原始的魏氏组织。然而明条纹区域受热循环作用明显, 高温使得原始组织中部分  $\alpha$  相长大, 其余部分  $\alpha$  相溶解转变成  $\beta$  相, 提高了  $\beta$  相含量<sup>[18]</sup>。随后, 新的  $\alpha$  相重新在  $\beta$  转变基体上析出。由于转变时  $\alpha$  相存在多种变体取向<sup>[19]</sup>, 且元素充分扩散, 最终形成  $\alpha$  片层相对粗大且交织的网篮组织。由于两区域组织片层间距差异较大, 因此在光学显微镜下呈现出明暗条纹。经电子束重熔后, 沉积钛合金表面获得组织均匀且厚度约 800  $\mu\text{m}$  的重熔层, 如图 2d 所示。无论是明条纹区域(见图 2e)还是暗条纹区域(见图 2f),

其沉积态组织均转变细针状马氏体  $\alpha'$ 。XRD 分析结果(见图 3)也显示, 重熔层的主要物相为马氏体  $\alpha'$ 。在电子束作用下, 明条纹与暗条纹区域表层重新熔化, 由于重熔处理时熔池冷却速度快 ( $>410$   $^{\circ}\text{C/s}$ )<sup>[16]</sup>, 此时高温  $\beta$  相发生马氏体相变, 即  $\beta \rightarrow \alpha'$ <sup>[17]</sup>, 得到马氏体  $\alpha'$  相。此外, 从 XRD 图谱上可以观察到, 重熔后的 Ti 衍射峰向右偏移。一方面, 由于 Al 原子半径 (0.143 nm) 和 V 原子半径 (0.132 nm) 均小于 Ti 的原子半径 (0.147 nm), 因此 Al、V 原子固溶后造成晶格收缩, 晶面间距减小, 使得衍射峰向高角度方向偏移<sup>[20-21]</sup>。另一方面, 重熔处理时快速冷却产生的应力作用导致表层晶格发生畸变, 同样引起衍射峰向高角度方向移动<sup>[22]</sup>。

### 2.2 纳米压痕力学性能

重熔前后钛合金表面不同区域的纳米压痕载荷–位移曲线如图 4 所示。由图 4 可见, 沉积钛合金暗条纹区域的压入深入低于明条纹区域, 但重熔层的压入深入更低, 说明电子束重熔处理后沉积钛合金表层的抵抗变形能力显著增强。由载荷–位移曲线获得的纳米硬度及弹性模量见表 2。沉积态明条纹和暗条纹区的纳米硬度分别为 2.8、3.3 GPa, 而重熔处理后, 明、暗条纹区域纳米硬度相当, 提升至 3.7~3.8 GPa。沉积状态组织由片状  $\alpha$  相与晶间  $\beta$  相组成, 其硬度与铸造态或锻造态硬度值相近。由于明条纹内部  $\alpha$  片层比暗条纹内部  $\alpha$  片层粗大, 根据 Hall-Petch 公式可知<sup>[23]</sup>, 片层间距越细, 强度越高, 因此暗条纹区域纳米硬度大于明条纹区域纳米硬度。重熔处理后, 获得大量的

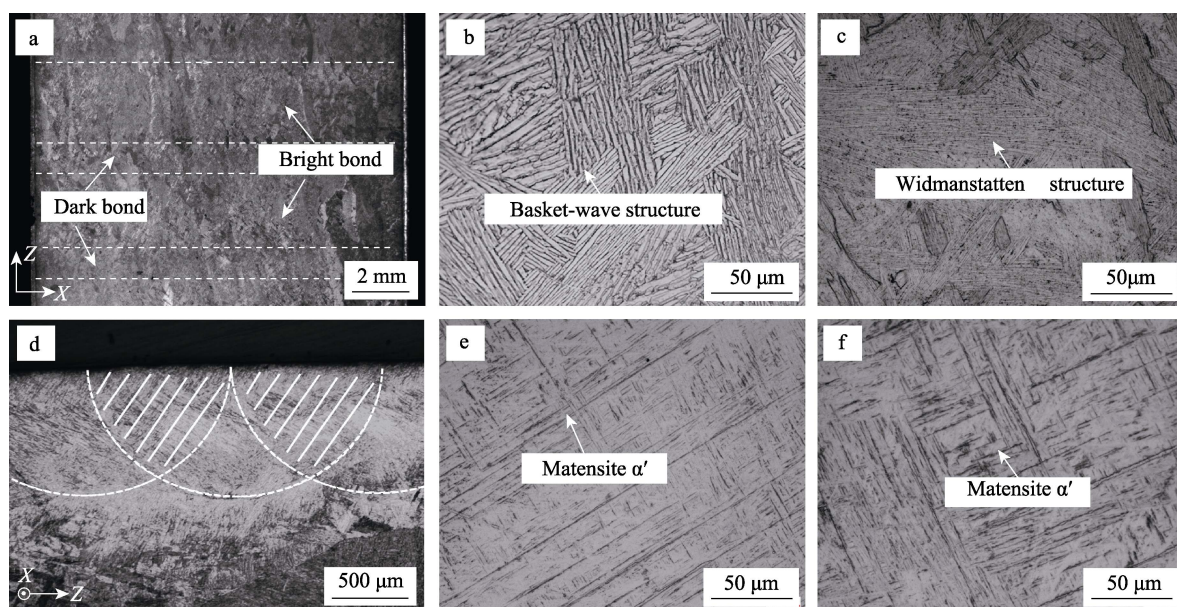


图 2 沉积钛合金宏观形貌 (a)、明条纹 (b) 和暗条纹微观形貌 (c)、

重熔层截面形貌 (d)、明条纹 (e) 及暗条纹重熔微观形貌 (f)  
Fig.2 Macrostructure of deposited alloy (a), microstructure of bright bond (b) and dark bond (c), and cross-sectional morphology of remelted layer (d), remelted microstructure in bright bond (e) and dark bond (f)

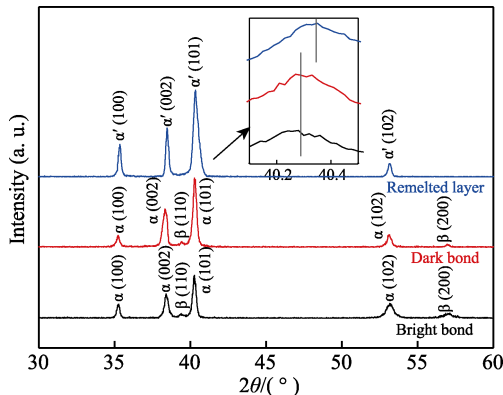


图3 电子束重熔前后钛合金表层的XRD图谱  
Fig.3 XRD patterns of surface structure over titanium alloy before and after electron beam surface remelting

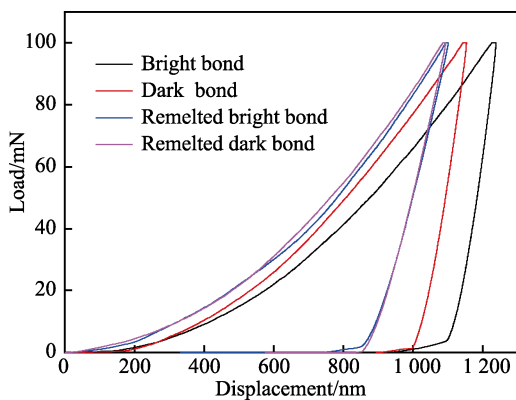


图4 重熔前后钛合金表面不同区域的载荷-位移曲线  
Fig.4 Loading-displacement curves of different regions on titanium alloy surface before and after remelting

细针状马氏体 $\alpha'$ 相是使沉积钛合金表面强化的重要原因。研究表明,材料纳米硬度和弹性模量的比值( $H/E_r$ )和 $H^3/E_r^2$ 比值可用于评估材料耐磨性能<sup>[24-26]</sup>,其中 $H/E_r$ 比值与弹性应变有关<sup>[24-25]</sup>,而 $H^3/E_r^2$ 比值表示材料抗塑性变形能力<sup>[26]</sup>。 $H/E_r$ 比值和 $H^3/E_r^2$ 比值越大,表明材料的抗磨损能力越强。与沉积钛合金明、暗条纹区域相比,重熔层的 $H/E_r$ 比值(0.031)和 $H^3/E_r^2$

表2 重熔前后钛合金表面不同区域纳米力学性能数据  
Tab.2 Nanomechanical properties of different regions on titanium alloy surface before and after remelting

	$H/GPa$	$E_r/GPa$	$H/E_r$	$H^3/E_r^2/GPa$
Bright band	$2.8 \pm 0.2$	$141 \pm 5$	$0.020 \pm 0.0007$	$0.0011 \pm 0.0002$
Dark band	$3.3 \pm 0.2$	$136 \pm 4$	$0.024 \pm 0.0008$	$0.0019 \pm 0.0002$
Remelted bright band	$3.7 \pm 0.1$	$121 \pm 3$	$0.031 \pm 0.0016$	$0.0035 \pm 0.0007$
Remelted dark band	$3.8 \pm 0.2$	$123 \pm 4$	$0.031 \pm 0.0006$	$0.0036 \pm 0.0003$

比值(0.0036)更高,表现出良好的硬弹性,说明重熔层能够提升沉积钛合金表面强韧度。因此,可预测重熔层具有更优的抗磨能力。

### 2.3 摩擦性能

重熔前后试样的摩擦系数曲线、平均摩擦系数及磨损率如图5所示。从图5a中可以看出,所有试样的摩擦系数在磨损初期均呈上升趋势。这是因为在预磨阶段,摩擦力和对磨面的粗糙度逐渐增大,使得摩擦系数也随之增大。经过一定时间的预磨后,可以发现试样摩擦系数逐渐趋于平稳,进入稳定磨损阶段。然而,未重熔试样在经历一段相对稳定磨损后,其摩擦系数继续上升,且出现较大的波动。这是由于未重熔样品表面组织的差异,在经历一段时间对磨后,出现不同程度的磨损,致使对磨面不平整,引起摩擦磨损过程不稳定,使得磨损加剧<sup>[11,27]</sup>。

从磨痕三维形貌图可以发现,未重熔试样磨痕面不平整,局部磨损严重,如图6a所示。对比可见,重熔试样磨痕面平整(见图6b),其摩擦磨损过程稳定。由图5b可知,重熔前后试样的平均摩擦系数分别为0.56、0.45,磨损率分别为 $4.61 \times 10^{-13}$ 、 $3.59 \times 10^{-13} \text{ mm}^3/(\text{N}\cdot\text{m})$ 。重熔处理后,试样的平均摩擦系数与磨损率分别降低了19.6%、22.1%,说明重熔处理提高了沉积钛合金表面的耐磨性能,与纳米压痕预测结果一致。重熔层具有优异的耐磨性主要源于其较高的硬

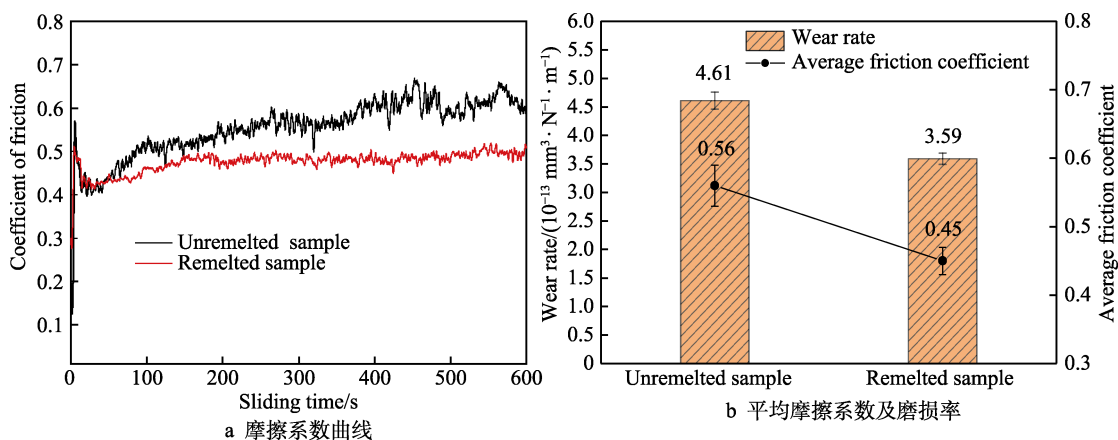


图5 重熔前后试样的摩擦系数曲线、平均摩擦系数及磨损率  
Fig.5 Friction coefficient curves (a), average friction coefficient and wear rate (b) of samples before and after remelting

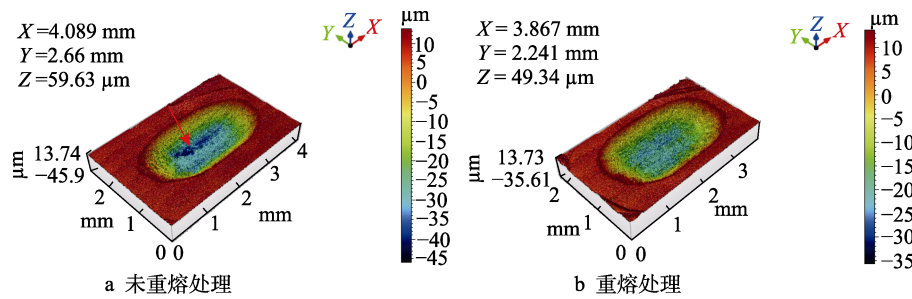


图 6 未重熔处理及重熔处理试样的磨痕三维形貌  
Fig.6 Three-dimensional morphologies of wear scars in un-remelted (a) and remelted (b) samples

度, 增强了沉积钛合金表面的磨损抗力。其次, 均匀的重熔组织保证了磨损的稳定性, 避免了局部磨损过快引起磨损加剧。

未重熔及重熔处理试样的磨损形貌如图 7 所示。从图 7 中可以看出, 2 种试样磨损表面均存在沿磨损方向的犁沟、剥落的氧化物层及粘着痕迹, 这些都是磨粒磨损、氧化磨损及粘着磨损的典型特征<sup>[8,27-28]</sup>。不同的是, 未重熔试样磨损表面犁沟较深且不均, 同时出现明显的塑性变形和大片粘着痕迹(见图 7a), 而重熔层磨损表面的犁沟较浅, 粘着痕迹较轻微(图 7b)。这是因为沉积钛合金表面硬度相对较低, 磨球易压入基体表面, 产生较多碎片而导致犁沟形成。此外, 摩擦过程产生大量的摩擦热。一方面, 由于钛元素活泼性强, 在摩擦热作用下, 被犁起的碎片极易与空气接触而生成氧化物<sup>[8,28]</sup>。另一方面, 由于沉积钛合金主要由片层  $\alpha$  相和  $\beta$  相组成, 其硬度较低, 变形

抗力不足, 在接触力作用下磨痕塑性变形严重, 摩擦热使周围材料软化, 使得对磨面在瞬间高温下发生粘着<sup>[27-28]</sup>。同时, 由于沉积钛合金内部明、暗条纹区域组织不均, 因此在磨损表面存在不同程度的损伤, 提高了对磨面粗糙度, 引起后期摩擦磨损过程不稳定(见图 5a), 从而加剧磨损<sup>[28]</sup>。经重熔处理后, 较快的冷却速度使得马氏体发生相变, 在沉积钛合金表面产生大量的细针状马氏体  $\alpha'$  相, 提高了表面硬度, 能够有效抵抗摩擦磨损过程接触变形, 增强摩擦抗力。因此, 重熔层磨痕表面的犁沟和粘着痕迹相对轻微。先前的研究结果<sup>[29-30]</sup>也证实, 较高硬度的马氏体  $\alpha'$  相比片层  $\alpha+\beta$  相表现出更优异的耐磨性能。同时, 重熔后的表层组织均匀, 提高了沉积钛合金与摩擦副间的摩擦稳定性, 因此重熔层磨损较均匀(见图 6b)。但由于摩擦热和塑性变形的作用, 其磨损表面同样发生氧化物剥落现象(见图 7b)。

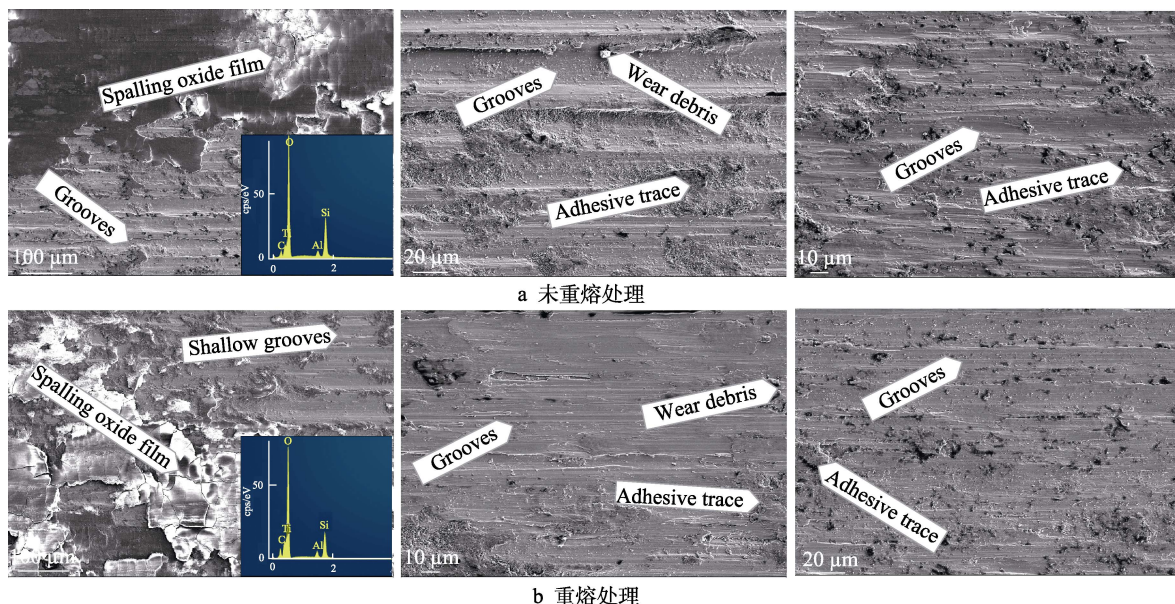


图 7 未重熔处理及重熔处理试样的磨损形貌  
Fig.7 Worn morphologies of un-remelted (a) and remelted (b) samples

### 3 结论

1) 电子束重熔处理能够显著改善熔丝沉积钛合金

沉积方向上的表面组织均匀性。经重熔处理后, 明条纹区域粗大片层的网篮组织( $\alpha+\beta$ )及暗条纹区域细长片层的魏氏组织( $\alpha+\beta$ )均转变成均匀分布的细针

状马氏体( $\alpha'$ )。

2)重熔处理使得沉积钛合金明、暗条纹区域的表层硬度变得均匀,且硬度提高至3.8 GPa,这是大量细针状马氏体 $\alpha'$ 相引起的强化结果。此外,重熔层表现出良好的硬弹性,有利于提升钛合金表面磨损抗力。

3)重熔处理后,钛合金的摩擦系数变得稳定,其平均摩擦系数为0.45,磨损率为 $3.59 \times 10^{-13} \text{ mm}^3/(\text{N}\cdot\text{m})$ ,与沉积钛合金相比,分别降低了19.6%、22.1%,主要发生磨粒磨损、氧化磨损及粘着磨损。

### 参考文献:

- [1] 张蕾涛, 刘德鑫, 张伟楠, 等. 钛合金表面激光熔覆涂层的研究进展[J]. 表面技术, 2020, 49(8): 97-104.  
ZHANG Lei-tao, LIU De-xin, ZHANG Wei-qiang, et al. Research Progress of Laser Cladding Coating on Titanium Alloy Surface[J]. Surface Technology, 2020, 49(8): 97-104.
- [2] 王欣, 罗学昆, 宇波, 等. 航空航天用钛合金表面工程技术研发进展[J]. 航空制造技术, 2022, 65(4): 14-24.  
WANG Xin, LUO Xue-kun, YU Bo, et al. Research Progress on Surface Engineering Technology of Aerospace Titanium Alloys[J]. Aeronautical Manufacturing Technology, 2022, 65(4): 14-24.
- [3] 巩水利, 锁红波, 李怀学. 金属增材制造技术在航空领域的发展与应用[J]. 航空制造技术, 2013, 56(13): 66-71.  
GONG Shui-li, SUO Hong-bo, LI Huai-xue. Development and Application of Metal Additive Manufacturing Technology in Aviation Field[J]. Aeronautical Manufacturing Technology, 2013, 56(13): 66-71.
- [4] 徐军强, 朱军, 范吉康, 等. 使用电子束自由成形制备Ti6Al4V合金的组织和力学性能[J]. 真空, 2019, 167: 364-373.  
XU Jun-qiang, ZHU Jun, FAN Ji-kang, et al. Microstructure and Mechanical Properties of Ti6Al4V Alloy Fabricated Using Electron Beam Freeform Fabrication[J]. Vacuum, 2019, 167: 364-373.
- [5] 锁红波. 电子束快速成形TC4钛合金显微组织及力学性能研究[D]. 武汉: 华中科技大学, 2014.  
SUO Hong-bo. Study on Microstructure and Mechanical Properties of TC4 Titanium Alloy by Rapid Electron Beam Forming[D]. Wuhan: Huazhong University of Science and Technology, 2014.
- [6] KOK Y, TAN X P, WANG P, et al. Anisotropy and Heterogeneity of Microstructure and Mechanical Properties in Metal Additive Manufacturing: A Critical Review[J]. Materials & Design, 2018, 139: 565-586.
- [7] TAO Xue-wei, YAO Zheng-jun, ZHANG Sha-sha. Reconstruction and Refinement of TiB Whiskers in Titanium Matrix Composite after Electron Beam Remelting[J]. Materials Letters, 2018, 225: 13-16.
- [8] 成前前, 万善宏, 易戈文, 等. Ti6Al4V表面激光改性层重熔处理的微观组织特征及宽温域摩擦学性能研究[J]. 摩擦学学报, 2022, 42(3): 470-481.  
CHENG Qian-qian, WAN Shan-hong, YI Ge-wen, et al. Microstructure Characteristics and Wide Temperature Range Tribological Properties of Ti6Al4V Laser Modified Surface by Remelting[J]. Tribology, 2022, 42(3): 470-481.
- [9] YAO Y, LI X, WANG Y Y, et al. Microstructural Evolution and Mechanical Properties of Ti-Zr Beta Titanium Alloy after Laser Surface Remelting[J]. Journal of Alloys and Compounds, 2014, 583: 43-47.
- [10] ZHANG Ting, FAN Qing, MA Xiao-li, et al. Effect of Laser Remelting on Microstructural Evolution and Mechanical Properties of Ti-35Nb-2Ta-3Zr Alloy[J]. Materials Letters, 2019, 253: 310-313.
- [11] 叶秀, 武美萍, 缪小进, 等. 激光重熔对Ti-6Al-4V选区激光熔化成形质量的影响[J]. 表面技术, 2021, 50(8): 301-310.  
YE Xiu, WU Mei-ping, MIAO Xiao-jin, et al. Influence of Laser Remelting on Forming Quality of Ti-6Al-4V Fabricated by Selective Laser Melting[J]. Surface Technology, 2021, 50(8): 301-310.
- [12] HE Bei, CHENG Xu, LI Jia, et al. Effect of Laser Surface Remelting and Low Temperature Aging Treatments on Microstructures and Surface Properties of Ti-55511 Alloy[J]. Surface and Coatings Technology, 2017, 316: 104-112.
- [13] CHEN Zi-jin, LIU Yong, WU Hong, et al. Microstructures and Wear Properties of Surface Treated Ti-36Nb-2Ta-3Zr-0.35O Alloy by Electron Beam Melting (EBM)[J]. Applied Surface Science, 2015, 357: 2347-2354.
- [14] KARIMI J, ANTONOV M, KOLLO L, et al. Role of Laser Remelting and Heat Treatment in Mechanical and Tribological Properties of Selective Laser Melted Ti<sub>6</sub>Al<sub>4</sub>V Alloy[J]. Journal of Alloys and Compounds, 2022, 897: 163207.
- [15] VAITHILINGAM J, GOODRIDGE R D, HAGUE R J M, et al. The Effect of Laser Remelting on the Surface Chemistry of Ti6Al4V Components Fabricated by Selective Laser Melting[J]. Journal of Materials Processing Technology, 2016, 232: 1-8.
- [16] TAN Xi-peng, KOK Y, TAN Yu jun, et al. Graded Microstructure and Mechanical Properties of Additive Manufactured Ti6Al4V via Electron Beam Melting[J]. Acta Materialia, 2015, 97: 1-16.
- [17] BAUFELD B, BRANDL E, VAN DER BIEST O. Wire Based Additive Layer Manufacturing: Comparison of Microstructure and Mechanical Properties of Ti-6Al-4V Components Fabricated by Laser-Beam Deposition and Shaped Metal Deposition[J]. Journal of Materials Processing Technology, 2011, 211(6): 1146-1158.
- [18] KELLY S M, KAMPE S L. Microstructural Evolution in Laser-Deposited Multilayer Ti-6Al-4V Builds: Part II. Thermal Modeling[J]. Metallurgical and Materials Transactions A, 2004, 35(6): 1869-1879.
- [19] HO A, ZHAO Hao, FELLOWES J W, et al. On the Origin of Microstructural Banding in Ti-6Al4V Wire-Arc Based High Deposition Rate Additive Manufacturing[J]. Acta Materialia, 2019, 166: 306-323.
- [20] TER HAAR G M, BECKER T H. Selective Laser Melting

- Produced Ti-6Al-4V: Post-Process Heat Treatments to Achieve Superior Tensile Properties[J]. *Materials* (Basel, Switzerland), 2018, 11(1): 146.
- [21] HE Jun-jie, LI Duo-sheng, JIANG Wu-gui, et al. The Martensitic Transformation and Mechanical Properties of Ti<sub>6</sub>Al<sub>4</sub>V Prepared via Selective Laser Melting[J]. *Materials* (Basel, Switzerland), 2019, 12(2): 321.
- [22] OSTAPENKO M G, SEMIN V O, D'YACHENKO F A, et al. Structure and Residual Stress Distribution in TiNi Substrate after Fabrication of Surface Alloy Using Electron-Beam Treatments[J]. *Acta Materialia*, 2022, 231: 117893.
- [23] 杜子杰, 李文渊, 刘建荣, 等. CMT 增材制造 TC4-DT 合金组织均匀性与力学性能一致性研究[J]. 金属学报, 2020, 56(12): 1667-1680.
- DU Zi-jie, LI Wen-yuan, LIU Jian-rong, et al. Study on the Uniformity of Structure and Mechanical Properties of TC4-DT Alloy Deposited by CMT Process[J]. *Acta Metallurgica Sinica*, 2020, 56(12): 1667-1680.
- [24] ZHANG Chao, ZHANG Bao-sen, XIE Li-shuai. Improving Mechanical Properties of Ni-W Based Nanocrystalline Films by Multilayered Architecture[J]. *Surface and Coatings Technology*, 2020, 402: 126341.
- [25] TAO Xue-wei, YAO Zheng-jun, ZHANG Sha-sha, et al. Investigation on Microstructure, Mechanical and Tribological Properties of In-Situ (TiB + TiC)/Ti Composite during the Electron Beam Surface Melting[J]. *Surface and Coatings Technology*, 2018, 337: 418-425.
- [26] ATTAR H, EHTEMAM-HAGHIGHI S, KENT D, et al. Nanoindentation and Wear Properties of Ti and Ti-TiB Composite Materials Produced by Selective Laser Melting[J]. *Materials Science and Engineering: A*, 2017, 688: 20-26.
- [27] 李明, 刘洋, 徐怀忠, 等. 固溶处理温度对激光选区熔化成型 Ti-6Al-4V 钛合金摩擦磨损性能的影响[J]. 材料热处理学报, 2019, 40(8): 39-49.
- LI Ming, LIU Yang, XU Huai-zhong, et al. Effect of Solid Solution Treatment Temperature on Friction and Wear Properties of Ti-6Al-4V Titanium Alloy Prepared by Selective Laser Melting[J]. *Transactions of Materials and Heat Treatment*, 2019, 40(8): 39-49.
- [28] 李新星, 施剑峰, 王红侠, 等. Ti6Al4V 合金干滑动磨损过程中摩擦层及摩擦氧化物的作用[J]. 表面技术, 2019, 48(12): 233-239.
- LI Xin-xing, SHI Jian-feng, WANG Hong-xia, et al. Role of Tribo-Layers and Tribo-Oxides in Dry Sliding Wear Process of Ti6Al4V Alloy[J]. *Surface Technology*, 2019, 48(12): 233-239.
- [29] BALLA V K, SODERLIND J, BOSE S, et al. Microstructure, Mechanical and Wear Properties of Laser Surface Melted Ti6Al4V Alloy[J]. *Journal of the Mechanical Behavior of Biomedical Materials*, 2014, 32: 335-344.
- [30] MARQUER M, LAHEURTE P, FAURE L, et al. Influence of 3D-Printing on the Behaviour of Ti<sub>6</sub>Al<sub>4</sub>V in High-Speed Friction[J]. *Tribology International*, 2020, 152: 106557.

责任编辑: 刘世忠

(上接第 146 页)

- [26] HUANG Shi-ming, SUN Da-qian, WANG Wen-quan, et al. Microstructures and Properties of In-Situ TiC Particles Reinforced Ni-Based Composite Coatings Prepared by Plasma Spray Welding[J]. *Ceramics International*, 2015, 41(9): 12202-12210.
- [27] UMANSKYI O, STOROZHENKO M, HUSSAINOVA I, et al., Effect of TiB<sub>2</sub> Additives on Wear Behavior of NiCrBSi-based Plasma-sprayed Coatings[J]. *Materials Science*, 2016, 22(1): 15-19.
- [28] HIGUERA H V, BELZUNCE V F J, MENENDEZ A C, et al. A Comparative Study of High-temperature Erosion Wear of Plasma-sprayed NiCrBSiFe and WC-NiCrBSiFe Coatings under Simulated Coal-fired Boiler Conditions [J]. *Tribology International*, 2001, 34(3): 453.
- [29] BABU P S, RAO D S, KRISHNA L R, et al. Weibull Analysis of Hardness Distribution in Detonation Sprayed Nano-structured WC-12Co Coatings[J]. *Surface & Coatings Technology*, 2017, 319: 468.
- [30] YANG Xiu-cong, LI Guo-lu, WANG Hai-dou, et al. Effect of Flame Remelting on Microstructure and Wear Behaviour of Plasma Sprayed NiCrBSi-30%Mo Coating [J]. *Surface Engineering*, 2018, 34(3): 279.
- [31] ZHANG Chun-yue, CHU Zhen-hua, WEI Fu-shuang, et al. Optimizing Process and the Properties of the Sprayed Fe-based Metallic Glassy Coating by Plasma Spraying[J]. *Surface & Coatings Technology*, 2017, 319: 3698.
- [32] YU He-long, ZHANG Wei, WANG Hong-mei, et al. Bonding and Sliding Wear Behaviors of the Plasma Sprayed NiCrBSi Coatings[J]. *Tribology International*, 2013, 66: 3602.
- [33] WANG Yu, LIU Qi, ZHENG Quan-sheng, et al. Bonding and Thermal-Mechanical Property of Gradient NiCoCrAlY/YSZ Thermal Barrier Coatings with Millimeter Level Thickness[J]. *Coatings*, 2021, 11(5): 3690.

责任编辑: 万长清